UAV Powered Cooperative Anti-interference MEC Network for Intelligent Agriculture

Chenkai Li, Weidang Lu(✉), Xiaohan Xu, Hong Peng, and Guoxing Huang

College of Information Engineering, Zhejiang University of Technology, Hangzhou 310023, China
luweid@zjut.edu.cn

Abstract. Mobile edge computing (MEC) provides computing resources for lots of Internet-of-things (IoT) devices in intelligent agriculture, improving the efficiency of agriculture. The energy harvesting efficiency of wireless power MEC system can be improved through combining unmanned aerial vehicle (UAV) technique. In this paper, we propose an UAV powered cooperative anti-interference mobile edge computing strategy for intelligent agriculture, in which IoT devices transmit their information through distinct subcarriers. Required energy for information transmission of UAV is minimized through optimizing power allocation. Simulation results demonstrate the performance of our proposed strategy.

Keywords: Wireless power transfer (WPT) · Mobile edge computing · Cooperation · UAV

1 Introduction

With the maturity and commercial deployment of Internet-of-Things (IoT), smart applications have been gradually applied to intelligent agriculture. Due to the explosive growth of IoT devices in intelligent agriculture systems, a variety of real-time environmental information needs to be collected for ensuring yield and quality, insufficient computing resources have become a problem [1, 2].

MEC technology is able to provide cloud computing services for IoT devices, and assist IoT devices in completing computation-intensive and time-critically tasks through wireless access networks [3]. However, inadequate battery supply for IoT devices can impact MEC performance severely. WPT is able to provide sustainable and low-cost energy supply for low-power mobile devices from radio frequency (RF) signals, greatly extending the standby time of mobile devices [4]. [5] studied a WPT collaborative MEC system, aim at minimizing the emission energy under the energy consumption and delay constraints. A binary computation offloading strategy for multi-user WPT based MEC networks was studied in [6], which maximized the total computing rate of the mobile device by optimizing transmission rate and computation selection mode.

IoT devices are usually located in remote areas in intelligent agriculture. If the IoT device exceeds the range of wireless communication during the communication process,

X. Wang et al. (Eds.): 6GN 2020, LNICST 337, pp. 298–307, 2020.
https://doi.org/10.1007/978-3-030-63941-9_22

it will cause the communication with MEC to fail [7]. Because of its highly flexible characteristics, UAVs have been widely used in a variety of scenarios [8]. Moreover, the energy transfer efficiency is improved through the UAV-assisted wireless power transmission structure to create a short-distance power transmission link in [9]. In [10], optimizing the power allocation and trajectory of UAVs which are equipped with MEC servers and provide services for multiple mobile devices within a limited range, minimizes the total consumed energy.

However, WPT enabled wireless communication networks are vulnerable to the double "near-far" effect. IoT device located far away from ET acquires less energy but needs to communicate for a long distance. Through cooperation between closer-device and farther-devices, communication performance can be improved. The cooperation of the devices in wireless powered communication was studied in [11] to surmount the double "near-far" effect, in which the closer-device uses the same channel to assist the farther-devices, causing interference.

In order to surmount the interference in the process of IoT devices' cooperation, we propose an UAV powered cooperative anti-interference mobile edge computing strategy for intelligent agriculture, where the IoT device which is closer to the UAV transmits the information of the farther IoT devices and its own information by utilizing distinct subcarriers.

2 System Model and Problem Formulation

2.1 System Model

The UAV powered MEC network consists of one UAV and two IoT devices IoD_1 and IoD_2. We assume that IoD_1 and IoD_2 need to accomplish computationally intensive latency critical tasks. IoD_1 and IoD_2 obtain energy from UAV through WPT method and use the harvested energy to accomplish their computation tasks with partial offloading. IoD_1 and IoD_2 transmit their tasks with half-duplex mode. We adopt a harvest-then-offload protocol for wireless powered computation offloading, which uses a block-based TDMA structure with the duration of each block being T seconds.

Let I_i and O_i denote the size of the input computation data and output data, respectively. Assuming the maximum tolerable delay time $T_i = T (i \in \{1, 2\})$ of IoD_1 and IoD_2 are the same. Since input data is much larger than output data, i.e., $O_i \ll I_i$. We just consider the time of the WPT and uplink offloading as the total latency of the proposed UAV powered MEC system.

The signal is OFDM modulated on K subcarriers, and the subcarrier set is denoted as $N = \{1, 2, \cdots, K\}$. In order to surmount the interference, IoD_2 utilizes first half of subcarriers $k \in G_I$ to relay the tasks of IoD_1 and the other half subcarriers $k \in \overline{G_I}$ to transfer its own offloading tasks to UAV, where $G_I \in N$ and $\overline{G_I} \in N$.

In the first period $\frac{T}{3}$, UAV transmits signal to IoD_1 and IoD_2 over subcarrier k with power p_k at the same time, which is equally allocated. The harvest energy of IoD_i is given by

$$E_h^i = \frac{T}{3} \sum_{n=1}^{K} v_i \gamma_{i,k} p_k, i \in \{1, 2\} \tag{1}$$

where v_i denotes the energy conversion efficiency at IoD_i, $\gamma_{i,k}$ denotes the channel power gain on subcarrier k from UAV to IoD_i.

In the second period $\frac{T}{3}$, IoD_1 uses harvest energy to send offloading task to IoD_2 with power $p_{1,k}$. The offloading task $L_{1,2}$ is given by

$$L_{1,2} = \frac{T}{3} B \sum_{k=1}^{K} \log_2\left(1 + \frac{p_{1,k}\gamma_{3,k}}{N_2}\right) \tag{2}$$

where B denotes the channel bandwidth of subcarrier, $\gamma_{3,k}$ denotes the channel power gain on subcarrier k from IoD_1 to IoD_2, and N_2 denotes the receiver noise power at the IoD_2.

The energy consumed by offloading tasks from IoD_1 to IoD_2 is given by

$$E_{\text{off}}^{1} = \frac{T}{3} \sum_{k=1}^{K} p_{1,k} \tag{3}$$

In the third period $\frac{T}{3}$, IoD_2 uses harvest energy to forward the IoD_1's offloading task to UAV over subcarrier $k \in G_I$ with power $p_{21,k}$. The offloading task $L_{2,1}$ is given by

$$L_{2,1} = \frac{T}{3} B \sum_{k \in G_I} \log_2\left(1 + \frac{p_{21,k}\gamma_{4,k}}{N_0}\right) \tag{4}$$

where $\gamma_{4,k}$ denotes the channel power gain over subcarrier k from IoD_2 to UAV, and N_0 denotes the receiver noise power at the IoD_2.

Meanwhile, IoD_2 sends its own offloading task to UAV over subcarrier $k \in \overline{G_I}$ with power $p_{22,k}$. The offloading task L_2 is given by

$$L_2 = \frac{T}{3} B \sum_{k \in \overline{G_I}} \log_2\left(1 + \frac{p_{22,k}\gamma_{4,k}}{N_0}\right) \tag{5}$$

The energy consumed by offloading tasks from IoD_2 to UAV is given by

$$E_{off}^{2} = \frac{T}{3}\left(\sum_{k \in G_I} p_{21,k} + \sum_{k \in \overline{G_I}} p_{22,k}\right) \tag{6}$$

Thus, the offloading tasks size of IoD_1 with the relaying of the IoD_2 is given by

$$L_1 = \min\left\{L_{1,2}, L_{2,1}\right\} = L_{2,1} \tag{7}$$

The rest of data $I_i - L_i$ need to be computed locally at IoD_i, which should satisfy

$$(I_i - L_i(\mathbf{p}))C_i/f_i \leq T \tag{8}$$

where C_i denotes the amount of computing resources required to calculate 1-bit input data, f_i denotes the CPU frequency.

The minimum offloading data of IoD_i is denoted as

$$L_i(\mathbf{p}) \geq M_i^+ \tag{9}$$

where $M_i = I_i - f_i T / C_i$, $(x)^+ = \max\{x, 0\}$.

The energy consumption of IoD_i for local computation is given by

$$E_{loc}^i = (I_i - L_i) C_i Q_i \tag{10}$$

where $Q_i = k_i f_i^2$, k_i is the effective capacitance coefficient, depending on the chip architecture.

Therefore, IoD_i's saving energy is denoted as

$$E_s^i(P_0, \mathbf{p}) = E_h^i - E_{off}^i - E_{loc}^i \tag{11}$$

where $\mathbf{p} = [p_{1,k}, p_{21,k}, p_{22,k}]$.

2.2 Problem Formulation

In order to minimize the transmission energy of the UAV, the power allocation is optimized under the time delay constraint and the task size constraint. The optimization problem is given by

$$\text{(P1)}: \min_{\mathbf{p}} P_0 \tag{12}$$

subject to

$$E_s^1(P_0, \mathbf{p}) \geq 0 \tag{13a}$$

$$E_s^2(P_0, \mathbf{p}) \geq 0 \tag{13b}$$

$$M_1^+ \leq L_1(\mathbf{p}) \leq I_1 \tag{13c}$$

$$M_2^+ \leq L_2(\mathbf{p}) \leq I_2 \tag{13d}$$

3 Optimal Solution

P1 can be equivalently converted into P2, which is given by

$$\text{(P2)}: \min_{\mathbf{p}} P_0 \tag{14}$$

subject to

$$P_0 \geq \frac{\sum_{k=1}^{K} p_{1,k} + \frac{3C_1Q_1}{T}\left(I_1 - L_{2,1}\right)}{v_1 \sum_{k=1}^{K} \gamma_{1,k}} \tag{15a}$$

$$P_0 \geq \frac{\sum_{k\in G_I} p_{21,k} + \sum_{k\in \overline{G_I}} p_{22,k} + \frac{3C_2Q_2}{T}(I_2 - L_2)}{v_2 \sum_{k=1}^{K} \gamma_{2,k}} \tag{15b}$$

$$m_1 \leq p_{21,k} \leq m_2 \tag{15c}$$

$$n_1 \leq p_{22,k} \leq n_2 \tag{15d}$$

where the value of m_1, m_2, n_1 and n_2 come from the equations $L_{2,1} = M_1^+$, $L_{2,1} = I_1$, $L_2 = M_2^+$, $L_2 = I_2$, respectively. Considering $M_1^+ \leq L_{1,2} \leq I_1$, the range of $p_{1,k}$ is $m_3 \leq p_{1,k} \leq m_4$.

Let

$$f = \sum_{k=1}^{K} p_{1,k} - C_1Q_1B \sum_{k\in G_I} \log_2\left(1 + \frac{p_{21,k}\gamma_{4,k}}{N_0}\right) \tag{16}$$

From (15a), we can see that when f reaches its maximum value, P_0 reaches its minimum value. Calculating the first derivation of f with $p_{1,k}$ and $p_{21,k}$, we can get

$$\frac{\partial f}{\partial p_{1,k}} = 1 \tag{17a}$$

$$\frac{\partial f}{\partial p_{21,k}} = -\frac{C_1Q_1B\gamma_{4,k}}{\ln 2\left(N_0 + p_{21,k}\gamma_{4,k}\right)} \tag{17b}$$

Therefore, we can draw the conclusion that f increase monotonically with $p_{1,k}$ and decrease monotonically with $p_{21,k}$.

Let

$$y = \sum_{k\in G_I} p_{21,k} + \sum_{k\in \overline{G_I}} p_{22,k} - C_2Q_2B \sum_{k\in \overline{G_I}} \log_2\left(1 + \frac{p_{22,k}\gamma_{4,k}}{N_0}\right) \tag{18}$$

From (15b), we can get that P_0 reaches its minimum value when y reaches its maximum value. Calculating the first derivation of y with $p_{21,k}$ and $p_{22,k}$, we can get

$$\frac{\partial y}{\partial p_{21,k}} = 1 \tag{19a}$$

$$\frac{\partial y}{\partial p_{22,k}} = 1 - \frac{C_2Q_2B\gamma_{4,k}}{\ln 2\left(N_0 + p_{22,k}\gamma_{4,k}\right)} \tag{19b}$$

We can find that y increase monotonically with $p_{21,k}$. When $p_{22,k} = p^*_{22,k} = \frac{C_2 Q_2 B}{\ln 2} - \frac{N_0}{\gamma_{4,k}}$, $\frac{dy}{dp_{22,k}} = 0$. Thus, we can conclude that y decreases with $p_{22,k}$ when $p_{22,k} < p^*_{22,k}$ and increases with $p_{22,k}$ when $p_{22,k} > p^*_{22,k}$.

The minimum value of P_0 can be given by

$$P_0 = \max\{P_{01}, P_{02}\} \tag{20}$$

where P_{01} and P_{02} are the minimum value of P_0 obtained from (15a) and (15b), respectively. By analyzing the relative value of $p_{21,k}$ and $p_{22,k}$ as follows, we can obtain both values of P_{01} and P_{02}.

Case 1. When $p_{21,k} = m_1$, the minimum value of P_{01} is given by

$$P_{01} = \frac{1}{v_1 \sum_{k=1}^{N} \gamma_{1,k}} \left[\sum_{k=1}^{N} m_4 + \frac{3C_1 Q_1}{T} \left(I_1 - M_1^+ \right) \right] \tag{21}$$

(**a**) When $n_1 \le p^*_{22,k} \le n_2$, the minimum value of P_{02} is given by

$$P_{02} = \max \left\{ \begin{array}{l} \dfrac{\sum\limits_{k \in G_I} m_1 + \sum\limits_{k \in \overline{G_I}} n_1 + \frac{3C_2 Q_2}{T} \left(I_2 - M_2^+ \right)}{v_2 \sum\limits_{k=1}^{N} \gamma_{2,k}} \\ \dfrac{\sum\limits_{k \in G_I} m_1 + \sum\limits_{k \in \overline{G_I}} n_2}{v_2 \sum\limits_{k=1}^{N} \gamma_{2,k}} \end{array} \right. \tag{22}$$

(**b**) When $p^*_{22,k} < n_1$, the minimum value of P_{02} is given by

$$P_{02} = \frac{\sum\limits_{k \in G_I} m_1 + \sum\limits_{k \in \overline{G_I}} n_2}{v_2 \sum\limits_{k=1}^{N} \gamma_{2,k}} \tag{23}$$

(**c**) When $p^*_{22,k} > n_2$, the minimum value of P_{02} is given by

$$P_{02} = \frac{\sum\limits_{k \in G_I} m_1 + \sum\limits_{k \in \overline{G_I}} n_1 + \frac{3C_2 Q_2}{T} \left(I_2 - M_2^+ \right)}{v_2 \sum\limits_{k=1}^{N} \gamma_{2,k}} \tag{24}$$

Case 2. When $p_{21,k} = m_2$, the minimum value of P_{01} is given by

$$P_{01} = \frac{\sum_{k=1}^{N} m_4}{v_1 \sum_{k=1}^{N} \gamma_{1,k}} \tag{25}$$

(**a**) When $n_1 \leq p_{22,k}^{*} \leq n_2$, the minimum value of P_{02} is given by

$$P_{02} = \max \begin{cases} \dfrac{\sum_{k \in G_I} m_2 + \sum_{k \in \overline{G_I}} n_1 + \frac{3C_2Q_2}{T}\left(I_2 - M_2^{+}\right)}{v_2 \sum_{k=1}^{N} \gamma_{2,k}} \\ \dfrac{\sum_{k \in G_I} m_2 + \sum_{k \in \overline{G_I}} n_2}{v_2 \sum_{k=1}^{N} \gamma_{2,k}} \end{cases} \tag{26}$$

(**b**) When $p_{22,k}^{*} < n_1$, the minimum value of P_{02} is given by

$$P_{02} = \frac{\sum_{k \in G_I} m_2 + \sum_{k \in \overline{G_I}} n_2}{v_2 \sum_{k=1}^{N} \gamma_{2,k}} \tag{27}$$

(**c**) When $p_{22,k}^{*} > n_2$, the minimum value of P_{02} is given by

$$P_{02} = \frac{\sum_{k \in G_I} m_2 + \sum_{k \in \overline{G_I}} n_1 + \frac{3C_2Q_2}{T}\left(I_2 - M_2^{+}\right)}{v_2 \sum_{k=1}^{N} \gamma_{2,k}} \tag{28}$$

4 Simulation Results

The channel is modeled as Rician fading, since the signal strength of the line-of-sight signal is stronger than that of the indirect signal, which is modeled as $\gamma_k = \sqrt{\frac{M}{M+1}}\tilde{f} + \sqrt{\frac{1}{M+1}}\hat{f}(k)$, where $M = 3, \tilde{f}$ denotes the line-of-sight deterministic factor, $\hat{f}(k)$ denotes the Rayleigh fading. The number of subcarriers is $K = 32$ and the total bandwidth is \$32\$ MHz. For simplicity, we set $v_i = 1.0$, $k_i = 10^{-28}$ and the receiver noise power $N_0 = N_2 = N$. The block time T = 0.3–0.5 s. The CPU frequency $f_i = 0.50$ GHz. The number of CPU cycles required per bit of data is $C_i = 1000$ cycle/bit.

Figure 1 shows the relationship between UAV's minimum transmit power and the blocking time T with different values of input data I_i when $N = 10^{-6}$ W. In this condition, the distance between UAV and IoD_1, UAV and IoD_2, and IoD_1 and IoD_2 are set to be $d_1 = 5$ m, $d_2 = 3$ m and $d_{12} = 3$ m, respectively. From Fig. 1, we can discover that as the size of the input calculation data increases, the minimum transmit power of the UAV increases as well. This is because the IoT devices consume more power to transmit data to UAV and compute locally as the input data size increases. We can also find in Fig. 1 that the minimum transmit power of UAV increases as T decreases. This is because in the case of shorter block time, in order to finish the transmission, the IoT devices require a higher transmission rate, which will lead to the UAV transmitting more power to provide energy for the IoT devices.

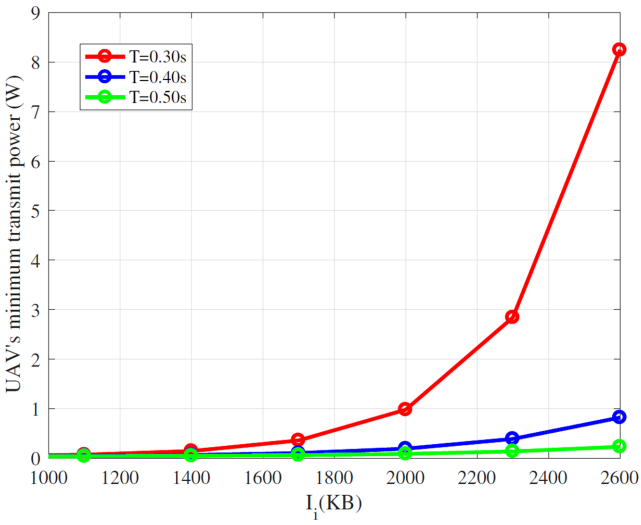

Fig. 1. Minimum transmit power of UAV versus T

Figure 2 shows the minimum transmit power of UAV versus noise power with different values of input data I_i when $T = 0.4$ s. In this condition, the distance parameters are set as same as Fig. 1. In Fig. 2, we can find that the minimum transmit power of UAV becomes smaller when the receiver noise power becomes smaller. That is because with a certain amount of offloading data, as shown in (2), the lower noise power, the lower power required.

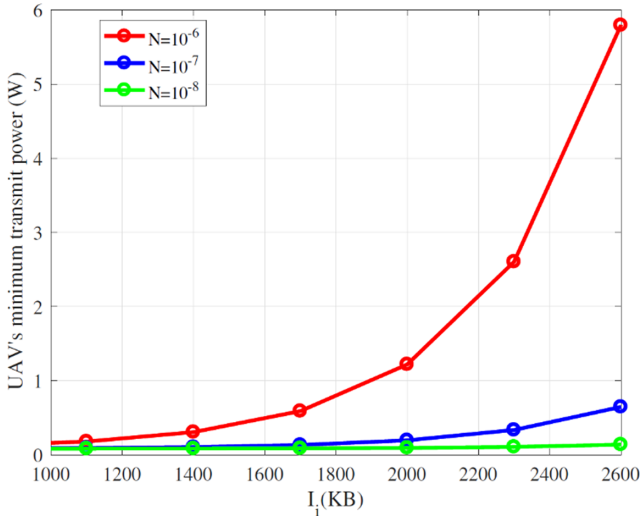

Fig. 2. Minimum transmit power of UAV versus *N*

5 Conclusion

In this paper, an UAV powered cooperative anti-interference mobile edge computing strategy is studied. To overcome the interference, utilizing the power harvested from the UAV broadcasting, different subcarriers was used by IoT devices to transmit the information to UAV for offloading. In addition, we formulate a power optimization problem. By optimizing the power allocation of IoT devices under the premise of meeting the delay and the scale of computing task, UAV's transmit power can be minimized. Simulation results prove the performance of the proposed strategy is effective and meets the expectation.

References

1. Lee, S., Oumaima, M., Ryu, S., Park, J.: A realtime spatiotemporal data acquisition system for precision agriculture. In: 2017 International Conference on Intelligent Environments (IE), pp. 149–152 (2017)
2. Bayrakdar, M.E.: A smart insect pest detection technique with qualified underground wireless sensor nodes for precision agriculture. IEEE Sens. J. **19**, 10892–10897 (2019)
3. Hua, M., Wang, Y., Li, C., Huang, Y., Yang, L.: UAV-aided mobile edge computing systems with one by one access scheme. IEEE Trans. Green Commun. Network. **3**, 664–678 (2019)
4. Wang, K., Yang, K., Chen, H., Zhang, L.: Computation diversity in emerging networking paradigms. IEEE Wirel. Commun. **24**, 88–94 (2017)
5. Zhang, K., et al.: Energy-efficient offloading for mobile edge computing in 5G heterogeneous networks. IEEE Access **4**, 5896–5907 (2016)
6. Bi, S., Zhang, Y.J.: Computation rate maximization for wireless powered mobile-edge computing with binary computation offloading. IEEE Trans. Wirel. Commun. **17**, 4177–4190 (2018)

7. Wang, S., Urgaonkar, R., He, T., Chan, K., Zafer, M., Leung, K.K.: Dynamic service placement for mobile micro-clouds with predicted future costs. IEEE Trans. Parallel Distrib. Syst. **28**, 1002–1016 (2017)
8. Hua, M., Yang, L., Li, C., Wu, Q., Swindlehurst, A.L.: Throughput maximization for UAV-aided backscatter communication networks. IEEE Trans. Commun. **68**, 1254–1270 (2020)
9. Zeng, Y., Zhang, R., Lim, T.J.: Wireless communications with unmanned aerial vehicles: opportunities and challenges. IEEE Commun. Mag. **54**, 36–42 (2016)
10. Zhang, T., Xu, Y., Loo, J., Yang, D., Xiao, L.: Joint computation and communication design for UAV-assisted mobile edge computing in IoT. IEEE Trans. Industr. Inform. **16**, 5505–5516 (2019)
11. Liang, H., Zhong, C., Suraweera, H.A., Zheng, G., Zhang, Z.: Optimization and analysis of wireless powered multi-antenna cooperative systems. IEEE Trans. Wirel. Commun. **16**, 3267–3281 (2017)